Numerical investigation on the impact of wind-induced hydraulics on dissolved oxygen characteristics in a shallow stormwater pond

Liyu Chen, Patrick M. D'Aoust, Colin D. Rennie, Alexandre Poulain, Frances Pick, Ru Wang and Robert Delatolla

ABSTRACT

Stormwater ponds (SWPs) are widely utilized for flood and water quality control. Low-flow rates are common in SWPs, sometimes causing wind-driven currents to become the dominant hydrodynamic force during ice-free periods. Hence, it is essential to understand the influence of the wind-induced flow on stratification and dissolved oxygen (DO) concentrations in shallow SWPs to predict the performance and water quality of these systems. The objective of this study is to evaluate the influence of wind-driven circulation on the spatial distribution of DO in an SWP using a numerical model. A bottom-mounted acoustic Doppler current profiler (ADCP) was utilized to measure small wind-induced currents and to validate a hydrodynamic model, which suggested that a wind-dominated circulation was generated even with the moderate wind speed. Countercurrents opposite in the direction to surface wind-generated flow were also present. The DO model demonstrated that complete mixing can be produced by higher wind speed, leading to fully oxic conditions throughout the water column (7.00 mg/L DO or higher), wherein low DO water at depth was carried to the surface by upwelling circulation and was possibly replenished during the surface transportation. This sheds some light on the impact of wind-induced mixing on the water quality in shallow SWPs.

Key words | acoustic Doppler current profiler, dissolved oxygen, MIKE 3, stormwater pond, wind-induced flow

Liyu Chen
Patrick M. D'Aoust (corresponding author)
Colin D. Rennie
Ru Wang
Robert Delatolla
Department of Civil Engineering,
University of Ottawa,
Ottawa K1N 6N5,
Canada
E-mail: *pdaous3@uottawa.ca*

Alexandre Poulain
Frances Pick
Department of Biology,
University of Ottawa,
Ottawa K1N 6N5,
Canada

INTRODUCTION

Wet stormwater ponds (SWPs) are widely utilized for flood and water quality control as they represent one of the best management practices to mitigate the impact of runoff from urbanized areas (Ontario Ministry of the Environment 2003; USEPA 2009). SWPs are commonly designed to be shallow enough to prevent excessive safety concerns from the local residents, anaerobic digestion and thermal stratification, yet ensure enough depth to minimize algal blooms or resuspension of bed materials by major storm events (USEPA 2009; McEnroe *et al.* 2012). A mean depth of approximately 1–3 m is considered appropriate to provide an acceptable environment and sufficient hydraulic retention time (HRT) (USEPA 2004). Based on both field (e.g., Delatolla & Babarutsi 2005; Kachhwal *et al.* 2012; Józsa 2014) and laboratory studies (Liang *et al.* 2006; Bentzen *et al.* 2008; Pattantyús-Ábrahám *et al.* 2008; Fabian & Budinski 2013; Khan *et al.* 2013), shallow water systems are clearly susceptible to wind-driven effects. In SWPs where minimal inflow is common, shallow ponds allow for wind-driven flow to become the dominant hydrodynamic force

doi: 10.2166/wqrj.2019.002

during ice-free periods (Pang *et al.* 2015; Andradóttir & Mortamet 2016). The momentum of the wind is partially transferred into the water column to produce waves, turbulence and large-scale circulation, whose generation does not require strong winds but may be generated by moderate winds. In particular, recent SWP hydraulic studies show that wind-driven flow speed and direction change with depth and that external surface forces are more efficiently transferred to the bottom of shallower ponds (Józsa 2014; Andradóttir & Mortamet 2016).

In SWPs, captured runoff is retained for an appropriate duration of time, and effluent characteristics are improved through physical, chemical and biological processes (Behera & Teegavarapu 2014). Good water quality in these ponds is essential not only to preserve the quality of the downstream receiving environments but also to ensure adequate aquatic habitats in wet facilities (Marsalek *et al.* 2005). The majority of stormwater retention pond quality studies focus on the chemical and biological characteristics of the ponds. Although some studies demonstrate the significance of hydraulic efficiency on SWPs with respect to pond shape, boundary configurations and topography (Jansons & Law 2007; Glenn & Bartell 2010; Zounemat-Kermani *et al.* 2015), very few studies have investigated the correlation between wind-driven hydraulic performance and detained stormwater quality. Dissolved oxygen (DO) is essential for the ecological environment and treatment performance in SWPs and can be strongly affected by waves, turbulence and large-scale circulation. As such, in the wind-induced flow-dominated SWPs, wind characteristics are likely to influence pond hydraulics and subsequently the spatial DO distribution and stratification. The objective of the present study is to evaluate the influence of wind-driven circulation on the spatial distribution of DO in an SWP using a three-dimensional numerical model.

Most previous DO computational models have considered SWPs to be a completely mixed compartment due to shallow bathymetry (German *et al.* 2003; Wium-Andersen *et al.* 2012). However, due to the complexity of the wind-driven flow affecting DO concentrations at different depths, the assumption of 'complete mixing' within SWPs does not always hold. Numerous previous studies have simplified simulation of the oxygen cycle in ponds and rivers. For example, Wium-Andersen *et al.* (2013) considered only photosynthesis/respiration and sediment oxygen demand (SOD), while Fan & Wang (2008) took only the process of biological oxygen demand (BOD) into consideration. However, DO is related to many environmental processes and parameters such as reaeration, photosynthesis/respiration, SOD, degradation of organic matter (e.g., BOD) and nutrient cycling. Moreover, these processes are likely to be specific to certain locations within the ponds, and the various parameters may vary spatially. Hence, a more complex model that incorporates all of the above-listed processes and parameters is desirable. Three-dimensional methods are better able to predict variation in depth of wind-generated current speed and direction than traditional two-dimensional depth-averaged computational methods. Thus, it is hypothesized that biochemical processes (such as sulphate reduction or ammonification) occurring at the water-sediment boundary may be more accurately predicted if wind-induced oxic conditions are tracked vertically through the water column.

In order to study wind-generated hydraulics and its influence on DO concentrations, a three-dimensional computational model was developed using MIKE 3 FM (DHI, Hørsholm, Denmark) for wind-driven hydrodynamics coupled with the ECOlab add-on. Full three-dimensional simulations with MIKE 3 allow computation throughout the whole water column, so that different characteristics such as current speed/direction and DO concentrations can be calculated at different depths. ECOlab simulates DO concentrations over time based on certain hydrodynamical conditions, while also considering the influence of reaeration by photosynthesis/respiration and oxygen-consuming processes such as BOD, SOD and nutrient cycling of ammonia, nitrite, nitrate and phosphorus.

The present study was conducted in an SWP in Ottawa, Canada. The hydrodynamic model was validated using velocity measurements taken by an ADCP (acoustic Doppler current profiler). To the best of the authors' knowledge, the stationary velocity measurements provided by a bottom-mounted ADCP were used for the first time to collect small wind-induced currents in an SWP. The water quality model was calibrated and validated using *in situ* samples taken on the same day as the velocity measurements. The major contributions of the study include: (i) visualized three-dimensional ADCP current results in

an SWP given the limitations of smaller water velocity magnitudes; (ii) three-dimensional wind-induced current and DO concentration simulation in an SWP using MIKE 3 and ECOlab with validated speed and direction; and (iii) an assessment of DO concentrations throughout the pond under different wind speed conditions.

MATERIALS AND METHODS

Study site description

This study was conducted at the Riverside South Stormwater Pond II (RSPII), a wet/retention SWP with a surface area of approximately 26,000 m^2, in a residential area of Riverside South, Ottawa, Canada. The pond was constructed in 2005 and is operated and maintained by Ottawa. Figure 1 shows the bathymetry of the RSPII as well as the locations of the measured ADCP stationary data points and DO sampling locations. The facility contains a large forebay with a maximum depth of 1.60 m, and the main body of the pond includes a 2.20 m deep trench extending from the southern end of the pond to the outlet at the northern end. The pond has a storage volume of 32,426 m^3 under normal water-level conditions and is designed to mitigate a 100-year storm event. The inlet structure is located at the southeast end of the pond with an average annual discharge of 0.003 m^3/s. The inlet structure houses a partially submerged 2,700 mm diameter trunk sewer and an elevated 1,350 mm diameter trunk sewer. The elevated trunk sewer saw limited usage at the time of the study as it serviced an area still under residential development. The HRT of RSPII, depending on the amount of precipitation and inflow, can range from 15 to 125 days. The pond drains into Mosquito Creek at the north of the facility through a 675 mm diameter reverse-sloped pipe designed to maintain a set permanent pool elevation. Several hydrogen sulphide (H_2S) production events have been reported at or around the facility since 2009, coinciding with periods of summer droughts and winter ice cover, during which poor water quality conditions were observed (D'Aoust *et al.* 2017; Chen *et al.* 2017). These events are associated with hypoxic conditions near the bed, and thus, a better understanding of mixing patterns in the pond is essential for the mitigation of H_2S production (Simpson 2001).

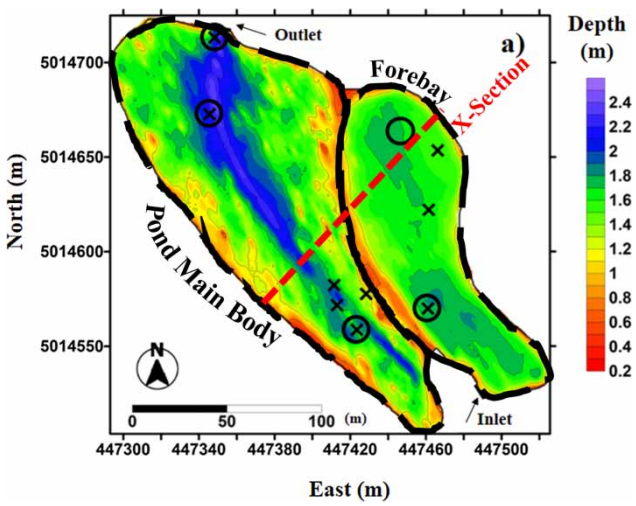

Figure 1 | ADCP data collection locations (x symbols) and DO sampling locations (circles) at the RSPII on 25 August 2015, with RSPII bathymetry (domain used in the MIKE 3 FM model), along with delineation of the pond forebay and main body regions and pond cross-section studied in Figure 9.

ADCP data collection

Velocity measurements were obtained using a SonTek RiverSurveyor® M9 (San Diego, CA) ADCP. This instrument was chosen due to its ability to measure water velocity over the whole water column in real time. A detailed description of ADCP usage techniques and terminology is available (Simpson 2001).

Velocity measurements were acquired on 25 August 2015, between 11:00 and 16:00 at the RSPII using the M9 ADCP at the sampling locations, as shown in Figure 1. At the time of measurements, the pond had experienced 4 days with little to no precipitation, and the last major rainfall (16.4 mm total precipitation) had occurred on 20 August 2015. At the low-flow velocities expected at RSPII, measurement noise caused by boat movement can mask measured velocities. To rectify this issue, a stationary bottom-mounted system was utilized for velocity data collection in this study. A Magellan ProMark3 Thales GPS unit with antenna (Santa Clara, CA) was used to record sampling locations. During velocity data collection, the ADCP unit was installed at the bottom of the pond, looking up, recording the vertical three-dimensional velocity profile from 0.45 m above the

bottom to the water surface. The boat was driven at least 2 m away from the collecting locations to mitigate the effect of boat movement on current velocity. Velocity profiles were recorded at 1 Hz for approximately 600 s at each location with a vertical resolution ranging from 0.02 to 0.06 m. One challenge of performing bottom-mounted data collection in a natural pond was abundant vegetation. Sampling locations were carefully selected, and the data were monitored in real time, to avoid the potential for macrophytes to cover or disturb the ADCP transducers. The bathymetry data of RSPII utilized in this study were provided by a bottom tracking collection of preliminary boat-mounted ADCP measurements acquired by Ottawa on 23 May 2013.

A MATLAB code developed by Rennie (Kachhwal *et al.* 2012) was modified and applied to process, filter and time and space average raw data to obtain mean velocity and direction within 10 cm depth cells in the water column. These profiles were plotted spatially in the pond using Tecplot 360 (Bellevue, WA). The ADCP data provided a visualized three-dimensional flow velocity profile at various locations in the pond, which help to understand the circulatory patterns in the RSPII under certain weather conditions.

Wind data collection

Wind speed and direction were obtained at the RSPII on 25 August 2015, using a HOBOware U30 Station wind logger (Bourne, MA) with a data recording frequency of 10 s. The wind anemometer was located at the inlet structure and securely fastened to a permanent railing at a height of approximately 10 m above the water surface to minimize wind disturbances and minimize local roughness effects. The wind data were collected on-site and compared with the data available from the Ottawa International Airport's (YOW) weather station (located approximately 4 km from the RSPII) to confirm modelling inputs.

Water quality sample collection

Field data for DO, BOD, chlorophyll-α (Chl-α), ammonia, nitrite, nitrate and total phosphorus (TP) were required as model inputs in this study. All sample measurements used in this study were acquired at RSPII at four specific depths (0.50, 1.00, 1.50 and 2.00 m below the water surface) at locations where it was feasible to do so on the same days and across the same general time period as the velocity and wind measurements. DO concentrations were taken *in situ* using a field optical YSI ProODO DO meter (Yellow Springs, OH). Water samples for BOD, chemical oxygen demand (COD), Chl-α, ammonia, nitrite, nitrate and TP testing were collected using a Wildco 1520 C25 Kemmerer Bottle 2.2 L TT water sampler (Yulee, FL). Tests were conducted using standard methods or equivalent, as outlined in Table 1. The COD/BOD ratio was obtained by testing 18 representative samples throughout the study period. This ratio was used to convert subsequent COD measurements into BOD values to benefit from more controlled experiments and faster laboratory turnaround times.

Laboratory kinetics study

Sediment samples were collected at the RSPII outlet using an Ekman dredge for laboratory kinetics testing. Laboratory results of the microbial kinetic experiments as described in detail by D'Aoust (2016) and D'Aoust *et al.* (2018) were utilized to determine the rates of change values, Arrhenius' temperature coefficient and half-saturation constants, which were then used as inputs for the MIKE 3 FM ECOlab model. Sediment samples for the experiments were harvested from the outlet of RSPII during fall of 2015. The Arrhenius temperature coefficient was determined for SOD and nitrification by analyzing the kinetic data acquired during laboratory testing. By plotting the change per unit of time of constituents versus time, the rate of change values of

Table 1 | Testing methods used for water quality parameters (APHA WEF 2012)

COD	Hach Method 8000 (equivalent to Standard Method 5220 D)
BOD	Modified Standard Methods 5210B
Chl-α	Modified Standard Methods 10200 H (with 95% ethanol extraction)
Ammonia	Hach Method 10205 (equivalent to Standard Method 4500-NH_3-B)
Nitrite	Standard Methods 4500-NO_2-B
Nitrate	Standard Methods 4500-NO_3-B
TP	Hach Method 8190 (equivalent to Standard Methods 4500-P E)

DO and ammonia concentrations was also obtained at 20 °C. The BOD, SOD and nitrification rates of changes were plotted against DO, and the resulting curve was utilized to determine half-saturation coefficients, as per Ghimire (2012).

NUMERICAL MODEL DEVELOPMENT

Hydrodynamic and water quality module

The three-dimensional hydrodynamic model MIKE 3 FM by DHI software (DHI 2012) was applied for RSPII pond flow simulation. MIKE 3 FM was developed specifically for applications within oceanographic, coastal and estuarine environments. Based on the small velocities inherent to RSPII, wind-driven flow may significantly contribute to the velocity profile of the pond. The model was chosen based on the capability of simulating three-dimensional flow as well as DO concentration throughout the entire water column when coupled with the ECOlab module (DHI 2017). Detailed information of the hydrodynamic model can be found in MIKE by DHI-MIKE 21 and MIKE 3 Flow Model FM Scientific Documentation (DHI 2012). The hydrodynamic model is based on the numerical solution of three-dimensional incompressible Reynolds-averaged Navier–Stokes equations invoking the assumptions of Boussinesq and hydrostatic pressure. In this study, sigma coordinates were used for the vertical mesh, where a σ-transformation was used for velocity components. Boundary shear stress was derived from the log-law. A cell-centred finite volume method was used for spatial discretization. The turbulent kinetic energy and the rate of dissipation of the turbulent kinetic energy are acquired from the $k-\varepsilon$ model (Rodi 2017). The eddy viscosity is calculated locally from $k-\varepsilon$. The model is capable of taking into consideration wind stress and evaporation/precipitation, and the open boundaries can be defined using water speed or elevation. Wind stress is developed from a drag formula (Wu 1980; Wu & Tsanis 1995) based on the wind speed.

The model considers the physical, chemical and biological interactions among ecosystem state variables, including the sedimentation of state variables. ECOlab is coupled to the Advection–Dispersion Modules of the DHI hydrodynamic flow models, so that transport mechanisms based on advection–dispersion can be integrated in the ECOlab simulation (DHI 2017). In this study, the model is used to assess the impact of wind-driven advection–dispersion on DO conditions, and in this specific model, oxygen balance is described as a function of reaeration, the biotic processes of photosynthesis and respiration, degradation of organic matter (decay of BOD), and the interaction with sediment (SOD) and nutrient cycling (nitrification of ammonia to nitrite and nitrite to nitrate). A general relation between DO and control parameters can be described as follows:

$$\mathrm{DO} = \text{reaeration} - \text{nitrification} - \mathrm{BOD} + \text{photosynthesis} - \text{respiration} - \mathrm{SOD}$$

Detailed information of the water quality model can be found in MIKE by DHI-Water Quality WQ Templates ECOlab Scientific Description (DHI 2012).

MIKE 3 model configuration and implementation

In order to simulate wind-driven flow in RSPII using MIKE 3 FM, a triangular computation mesh was generated (average grid spacing of approximately 4.0 m) coupled with 10 unevenly spaced σ-levels (layers) in the vertical direction. Open boundaries were manually designated at the inlet and the outlet based on the bathymetry and coordinates of inlet and outlet structures of the RSPII.

An annual discharge of 0.003 m^3/s was set for the inlet and outlet of the pond, based on the level of the pond during the field investigation. The pond boundary was set as a land boundary where normal velocity is equal to zero. To maintain the permanent pool level in the model similar to those observed at the SWP, a 4.00 m width by 0.50 m height trapezoidal weir with a bottom width of 2.00 m was created at 2.00 m above the bed to retain similar water level in the system at the outlet boundary, where fluid entry through the boundary was prevented. A horizontal 1.00 m diameter circular culvert was set up at 0.50 m above the bed to simulate the inlet condition. The initial hydrodynamic conditions in the model were applied using the final stage condition of a preliminary run without wind

add-on. Density was defined as a barotropic fluid. Wind speed and direction were applied using the data collected on the same day as the ADCP measurements within the whole running period from 7:00:00 to 16:43:20 on 25 August 2015. The drag coefficient of wind in this model was calibrated as demonstrated by Geernaert & Plant (1990). Precipitation was obtained using the data from the Ottawa International Airport weather station (Environment Canada Atmospheric Environment Service 2016), and the evaporation rate was estimated using Ferguson *et al.* (1970). In total, the model was run with 3,500 time steps and time intervals of 10 s, for a total run time of 9.72 h. Mesh and time step independence tests were conducted to confirm that the mesh was sufficiently resolved for the modelled flow. With this specific set-up, the Courant number was approximately 0.02, which was within the software recommended value (DHI 2012). Table 2 shows more detailed information of domain characteristics.

Water quality measurements at the RSPII on 25 August 2015 were set as initial conditions to initiate the model simulation. Likewise, boundary conditions of concentrations of water quality parameters were based on *in situ* samples in proximity to the inlet and the outlet at the RSPII. Measured concentrations of BOD, ammonia, nitrite, nitrate and TP on the simulation day were entered as initial and boundary conditions (Table 3). The concentrations of these parameters were relatively constant throughout the study period and had somewhat predictable patterns, which indicated relative representative conditions within the RSPII pond. The model does not simulate macrophytes at the bed and in proximity to the pond's exterior boundaries, which could contribute to the fluctuation of DO concentrations via photosynthesis and respiration. As such, Chl-α concentrations were adjusted to higher values (as shown in Table 3) for both initial and boundary conditions to simulate the contribution generated by macrophytes on 25 August 2015, at the RSPII. The inflow concentration of Chl-α was set to the seasonal average of 0.02 mg/L of RSPII; the initial and outlet concentrations were adjusted, respectively, to 0.60 and 0.20 mg/L to compensate for inadequate simulation of photosynthesis and respiration from vegetation. However, it should be mentioned that no literature has been found to support this assumption specifically for MIKE 3 Chl-α inputs. Values of state variables of both initial condition and boundary condition are listed in Table 3. These values were obtained empirically from trial and error exercises when calibrating the model with the real-life data.

Table 2 | MIKE 3 domain characteristics

Parameters	Model input
Elements	2,118
Nodes	1,138
Precipitation (daily average)	4.0 mm/day
Evaporation	9.6×10^{-1} mm/day
Wind friction	2.0×10^{-3} N/m^2

Table 3 | Initial and boundary inputs of ECOlab simulation in MIKE

Variable	Initial condition (mg/L)	Inlet boundary (mg/L)	Outlet initial condition (mg/L)
DO	10.0	10.0	10.0
BOD	1.0	2.0	2.0
Chl-α	6.0×10^{-1}	2.0×10^{-2}	2.0×10^{-1}
Ammonia-N	5.0×10^{-2}	5.0×10^{-2}	5.0×10^{-2}
Nitrite-N	9.0×10^{-4}	5.0×10^{-4}	5.0×10^{-4}
Nitrate-N	7.0×10^{-1}	8.0×10^{-1}	8.0×10^{-1}
TP	2.0×10^{-2}	2.0×10^{-2}	4.0×10^{-2}

The constants of environmental processes in MIKE 3 ECOlab were obtained from laboratory kinetic experiments. The soluble biochemical oxygen demand (sBOD) remained low and constant throughout the whole study period with a first decay rate of 0.48 mg/L per day at 20 °C obtained in the laboratory, which was similar to the value reported by Tu *et al.* (2014) on a constructed wetland in Taiwan. The half-saturation oxygen concentration of sBOD was 1.37 mg/L. Nitrification is modelled as the process of ammonia oxidation to nitrite and nitrite oxidation to nitrate. The first decay rate of overall nitrification of 0.17 mg/L per day at 20 °C was also acquired via laboratory experimentation. The rate of ammonia oxidation was kept the same as the nitrification rate as oxic systems do not accumulate nitrite under normal operations. Compared with the study by Tu *et al.* (2014), the RSPII has a relatively low ammonia/nitrite removal efficiency. Moreover, the temperature coefficient

for the nitrification decay rate of 1.088 and temperature coefficient for SOD of 1.150, along with the half-saturation oxygen concentration of nitrification and SOD of 0.48 and 3.51 mg/L, respectively, were also obtained from laboratory results.

SOD is composed of chemical SOD and biological SOD (Wang 1980). It is evident that the biological activity varies geographically and spatially within a pond due to varying benthic conditions. To account for the availability of spatially distributed carbon in sediment, the SOD per square metre parameter was varied spatially to incorporate the mass flux of carbon into the kinetic rate. Therefore, higher values of SOD per square metre of 3.00–5.00 g/m^2/day were utilized in the forebay due to the higher carbon input contributed by abundant sedimentation (USEPA 2004) and the population of microorganisms (Wang 1980). Likewise, lower SOD per square metre of 0.00–2.00 g/m^2/day were used in the main pond body according to the laboratory result of 1.75 g/m^2/day, obtained from water-sediment kinetic experiments. This assumption was furthermore supported by the literature. Rong & Shan (2016) reported that the SOD per square metre (20 °C) of two rivers in China ranged from 0.0 to 2.0 g/m^2/day. A lake in Illinois, USA, studied by Butts & Evans (1979) showed higher SOD concentrations (20 °C) of between 2.0 and 7.0 g/m^2/day.

Water transparency is essential to sustaining algae populations within the water column, and Secchi disk depth is a commonly used parameter to characterize optical properties (Tilzer 1988). Spatially non-uniform Secchi disk depths proved to be important in successful modelling of the complex spatially variable environmental conditions of RSPII. According to Jamu *et al.* (1999), Chl-α showed a negative correlation with Secchi disk depths due to its positive linear regression with overall light extinction coefficient. Secchi disk depths were assumed with an average of 0.50 m in the forebay and around 1.80 m in the main body, considering the change of turbidity due to different concentrations of sediment within the water column. These modifications are supported by the literature, which also mention that Secchi disk depths were also correlated with algal levels (Canfield & Hodgson 1983). The forebay had substantially more algae present than the main body of the pond for most of the study period.

Photosynthesis and respiration processes were described relative to a given maximum production at noon and the respiration rate. A 3:1 ratio of maximum oxygen demand at noon versus respiration rate of plants was obtained from Mérette (Rolon dos Santos Mérette 2012); values were set as 10 g/m^2/day for maximum production at noon and 3 g/m^2/day for the respiration rate. Essential constants of the DO model are listed in Table 4, including default values, values measured in the laboratory and parameters used for model calibration guided by literature values.

RESULTS AND DISCUSSION

In situ ADCP collected flow coupled with wind measurements

Understanding of the wind-induced flow in SWPs is necessary to understand mixing processes that influence the water quality. Figure 2 shows wind speed and direction within the ADCP sampling period from 7:00 to 18:00 at the RSPII on 25 August 2015. Average wind speed of 2.30 m/s and with a direction of 229.00° was observed. Comparing with the historical wind data from the Ottawa International Airport, moderate wind speed occurred on 25 August 2015. In this study, a high-wind day and a low-wind day were defined as the average wind speed of 4.30 and 1.10 m/s, based on an analysis of the wind speed data of 2015 measured within the same time range as the ADCP measurements.

Figure 3 demonstrates three-dimensional vector plots of ADCP-measured current velocity and direction at the RSPII on 25 August 2015, with bathymetry and an approximate average wind direction viewed in different angles. Easting and Northing are presented as the x- and y-axes, and the z-axis represents the pond depth in this figure. The measured velocities show an average magnitude of approximately 1.0 cm/s at all locations at the RSPII, with standard error in measured horizontal velocities less than 0.10 cm/s. A study on Lake Okeechobee, Florida, USA (Jin & Ji 2004) reported the wind-produced flow velocity can range from 0.00 to 40.00 cm/s in a lake with an approximate depth of 2.70 m with an average wind speed of 5.00 m/s. Moreover, Kachhwal *et al.* (2012) demonstrated that with an average wind speed of more than 7.00 m/s, a velocity magnitude of order 5.00 cm/s can be generated in the Shebandowan Mine tailings storage facility, Ontario, Canada, where only

Table 4 | Essential constants of environmental processes in MIKE 3 ECOlab

Description	Values	Source
Oxygen processes		
Temperature coefficient for respiration	1.08	Default
Half-saturation coefficient for respiration	2.00 mg/L	Default
Temperature coefficient for SOD	1.15	Measured
Half-saturation coefficient for SOD	3.51 mg/L	Measured
SOD per square metre	Spatially distributed	Measured/calibrated
Maximum oxygen production at noon, m^2	10/day	Calibrated
Respiration rate of plants, m^2	3/day	Calibrated
Secchi disk depths	Spatially distributed	Calibrated
BOD processes		
First-order decay rate at 20 °C (dissolved)	0.48/day	Measured
Temperature coefficient for decay rate (dissolved)	1.07	Default
Half-saturation oxygen concentration	1.37 mg/L	Measured
Nitrification		
First-order decay rate at 20 °C for ammonia to nitrite	0.17/day	Measured
First-order decay rate at 20 °C for nitrite to nitrate	0.17/day	Measured
Temperature coefficient for decay rate	1.088	Measured
Half-saturation oxygen concentration	0.48 mg/L	Measured
Oxygen demand by ammonia oxidation	3.42 g O_2/g NH_4-N	Default
Oxygen demand by nitrite oxidation	1.14 g O_2/g NH_4-N	Default
Chl-α processes		
Carbon to oxygen ration at primary production	0.2857 mg C/mg O	Default

the wind-driven flow existed. Although the collected current velocities were generally small in this study, velocity magnitude at the RSPII falls within similar order as those of Lake Okeechobee and the Shebandowan Mine tailings pond. The bathymetry utilized for the modelling had several smaller peaks throughout the pond, which could have had some small effects on the modelling, potentially lowering modelled velocities. Furthermore, vegetation present in the pond at the time when the ADCP data were collected may have slowed down water flowing through the pond, potentially influencing results.

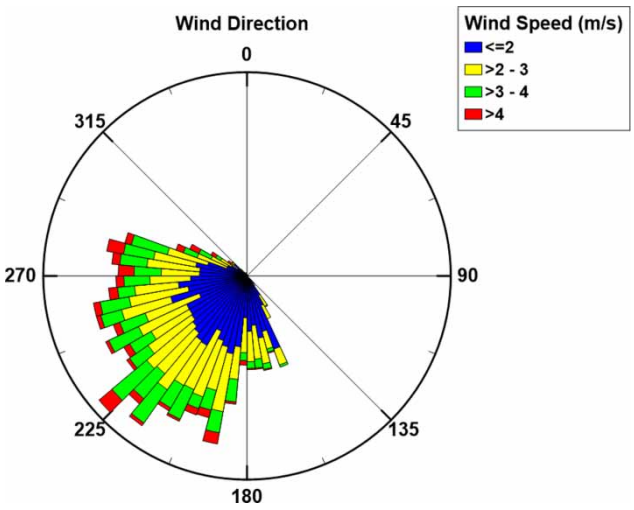

Figure 2 | Wind speed and direction during ADCP data collection measured at the RSPII.

Currents near the water surface (Figure 3) were observed to be in the downwind direction. This suggests wind conditions on 25 August 2015, generated enough momentum to generate surface current moving downwind. Wind-induced currents gradually changed direction towards the pond bottom (Figure 3), indicating that complex circulation patterns were created at different depths due to a non-linear interaction between currents (Signell *et al.* 1990). Moreover, countercurrent flow in the opposite

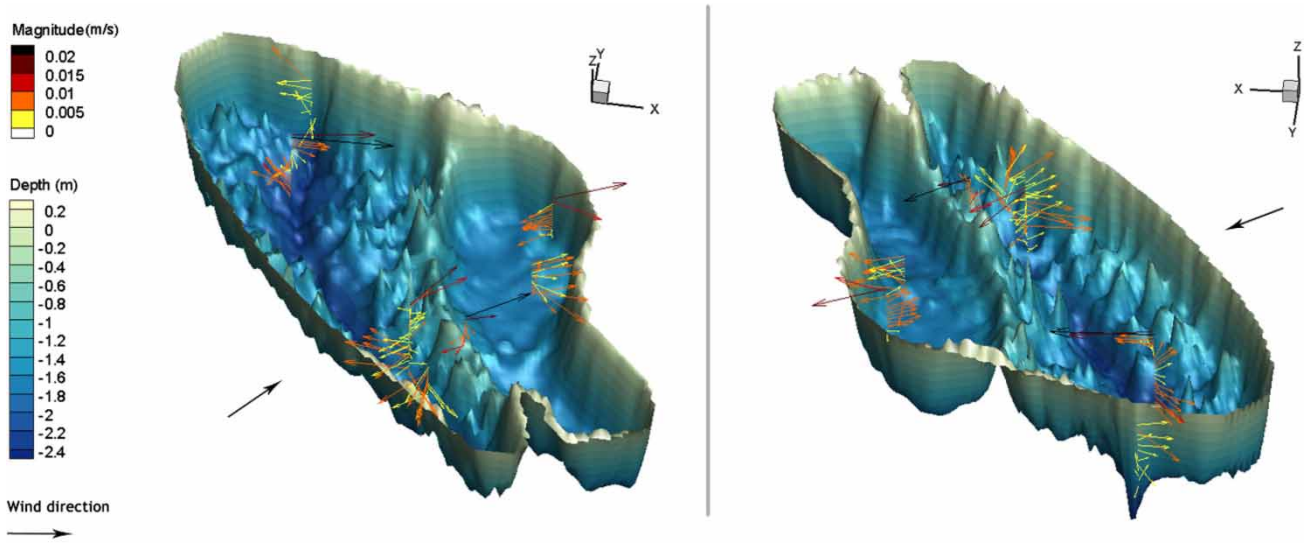

Figure 3 | Three-dimensional visualization of velocity magnitude and direction pattern of current flow at the RSPII with bathymetry and an approximate average wind direction viewed from different angles.

direction was observed near the bottom at some locations. Higher velocities were mainly observed close to the surface of the pond. Velocities collected close to the outlet facility of RSPII were smaller at all depths (less than 0.50 cm/s), where higher and more constant velocities were expected due to the discharge. These observed characteristics of velocity magnitudes and current directions support the assumption of wind being the most important driving force of the flow at RSPII during non-ice-covered conditions. Both the studies by Dumas *et al.* (2012) and Dufresne *et al.* (2014) suggest that wind directions are essential to driving overturning circulation that leads to efficient mixing. The ADCP results demonstrate the significant influence that can be exerted on mixing in RSPII under the wind directions observed on 25 August 2015. In the Ottawa region, as measured at Ottawa International Airport, more than 50% of windy days (defined as daily maximum wind speed over 8.60 m/s) were with wind directions from 170° to 290° between May and October 2015. These observations suggest that the dominant southwesterly wind can influence RSPII circulation during the summer period, based on the pond location and geometry.

Model validation and verification

Simulated results of the hydrodynamic model were validated using the ADCP-measured flow data on 25 August 2015 at the RSPII. Figure 4 illustrates a reasonable agreement between sampled and simulated values of velocity magnitudes and a reasonable agreement between the sampled and the simulated values of flow directions. Although the regression coefficient of determination (r^2) of velocity magnitude was small, the lower and upper 95% confidence slopes of 0.33 and 0.69 still showed a significant correlation between the observed and simulated velocity magnitudes (Figure 4(a)). Table 5 shows the statistics of the correlation plots. Given that the velocity magnitudes of both observed and simulated results were very small, the mean absolute error of simulated velocities (ϵ_a) seemed reasonable. The average discrepancy ratio (d) was 1.62, which showed a general overprediction (positive bias) of simulated velocity magnitude. Although underprediction was observed with lower velocity magnitudes, overprediction occurred with higher velocity magnitudes, and approximately 84% of the observed velocity magnitudes fell within $0.75 < d < 1.33$. Linear regressions assume that all error occurs in the y variable by minimizing the sum of square errors vertically from the regression line, while a principal axis functional relation describes the relation between x and y variables by minimizing the error on both axes (Rennie & Villard 2004). Figure 4(a) demonstrates that a functional relation better describes the relation between observed and simulated velocity magnitudes. The

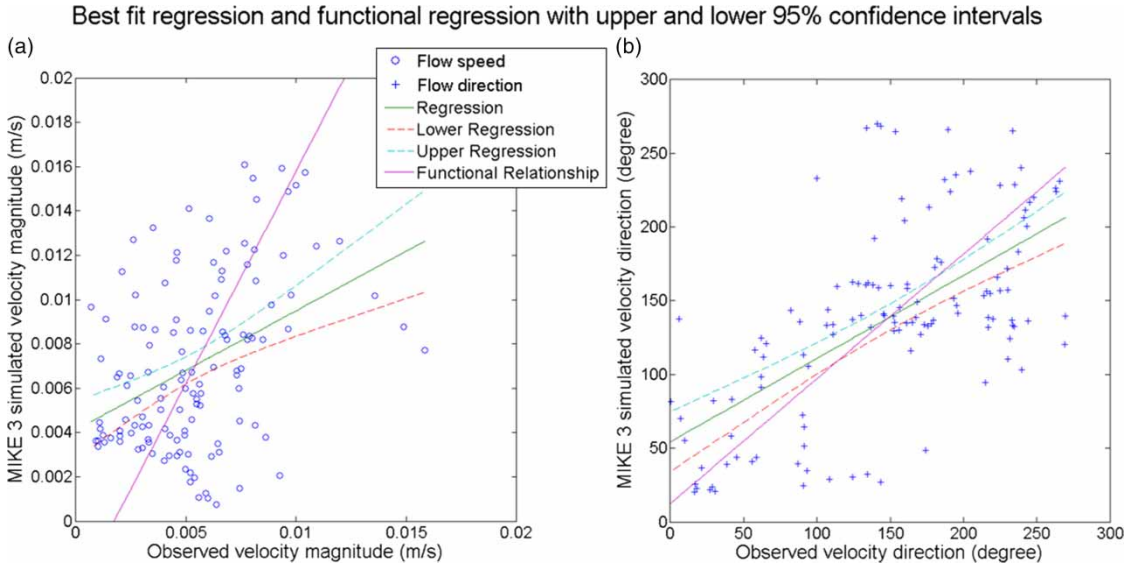

Figure 4 | Scatter diagrams of observed versus simulated (a) velocity magnitudes and (b) flow directions with linear regression and functional relation. Upper and lower 95% confidence bounds on the regressions are shown by dashed lines.

Table 5 | Statistics analysis of observed against simulated velocity magnitudes and flow directions

Measured versus simulated	r^2	ε_a	ε_{rms}	d_{min}	d_{max}	d_{avg}	$0.5<d<2.0$ (%)	$0.75<d<1.33$ (%)
Velocity magnitude (m/s)	0.17	0.0032	0.0041	0.12	6.57	1.62	0.89	0.84
Velocity direction (°)	0.39	41.57	60.08	0.19	23.34	1.29	0.86	0.52

functional relation slope was greater than 1:1 by 45°, which supports the finding of overestimation of larger velocity magnitudes.

Simulated and observed flow directions were better correlated than velocity magnitudes with a higher r^2 and 95% confidence upper slope of 1.01 and 0.70 lower slope (Figure 4(b)). Both ε_a and the root mean error (ε_{rms}) were less than 40% of the mean flow direction. Moreover, the mean discrepancy ratio (d_{avg}) was 1.29, and more than 85% of the velocity directions were within the range of $0.50 < d < 2.00$. The functional relation slope of wind direction was fairly close to 1, demonstrating that a well-correlated relation was established between observed and simulated results. In proximity to the pond surface, at more than half of the sampling locations, both observed and simulated velocity directions ranged from 15 to 55°, i.e., in the downwind direction. An average velocity direction of 200° was observed at depth, which indicated that the countercurrent flow occurred near the bottom of the pond. Overall, the model was shown to be capable of simulating small flows and wind-produced current in an oblong-shaped stormwater retention pond such as RSPII. Furthermore, the study also serves to generate an original database, which could benefit from additional days of sampling with various wind conditions.

The water quality model was validated using DO readings collected on 25 August 2015, and the results are shown in colour maps interpolated and plotted using Surfer® 11 by Golden Software, LLC (Figure 5), where high concentrations of DO are indicated as red, low concentrations as blue and very low concentrations as purple. Although the limited DO data were collected *in situ* due to restricted sampling time for carrying out both velocity and DO measurements on the same day, a very strong correlation was still established as demonstrated by r^2 of 0.70 (Figure 6). Both underestimations and overestimations were generated with higher DO concentrations due to the difficulty and complexity of environmental process modelling, such as the non-homogenous water environment, over-simplified description of mathematical formulations

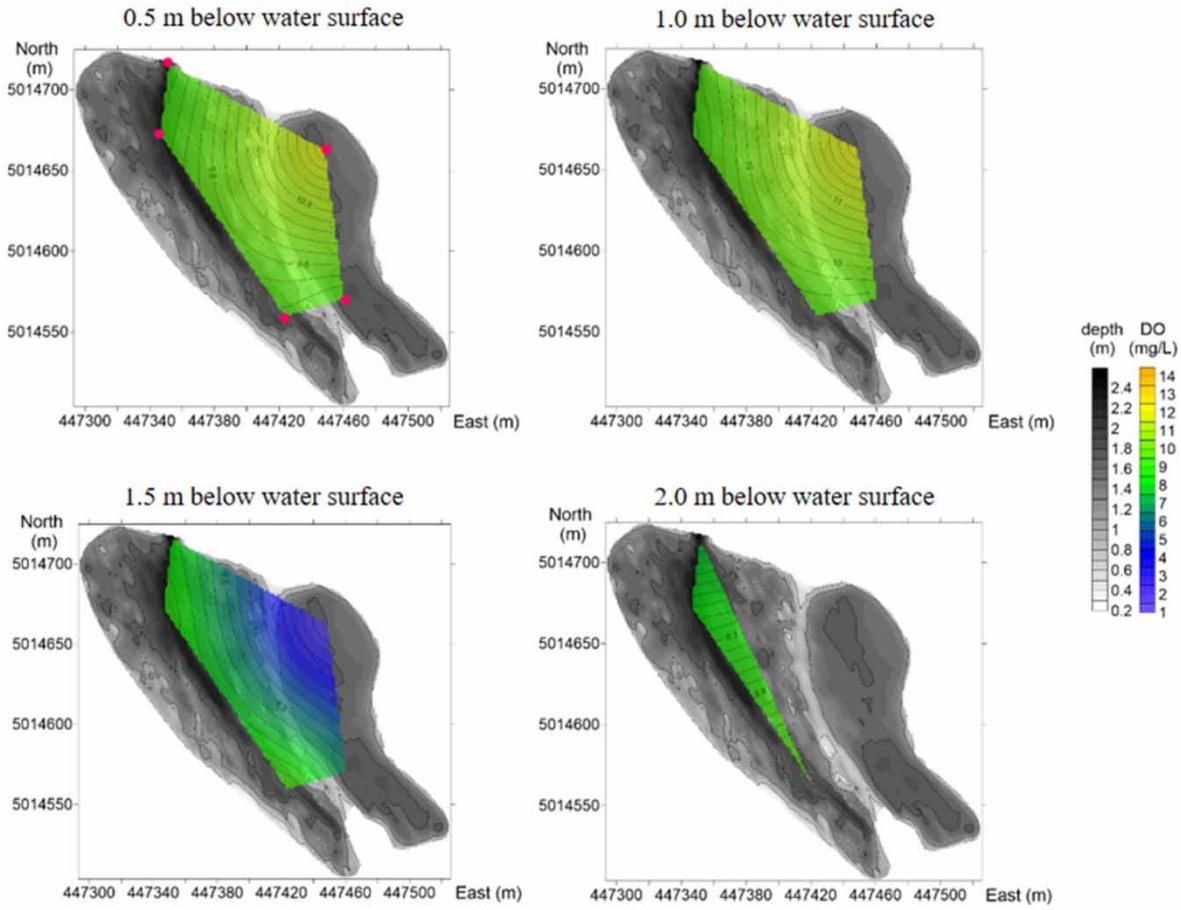

Figure 5 | DO concentrations at five locations at 0.5, 1.0, 1.5 and 2.0 m below the water surface at the RSPII on 25 August 2015. Please refer to the online version of this paper to see this figure in colour: http://dx.doi.org/10.2166/wqrj.2019.002.

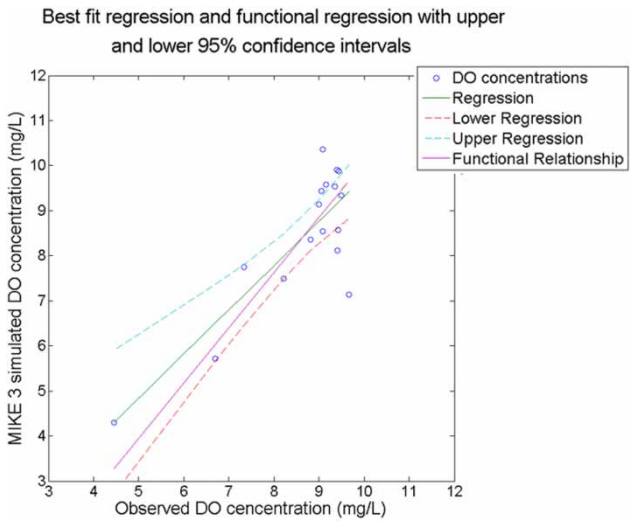

Figure 6 | Scatter diagram of observed versus simulated DO concentrations with linear regression and functional relation; perfect agreement is shown as the dash line.

and the uncertainty of vegetation simulation. However, linear regression slope and functional relation slope of 0.98 and 1.22, respectively, showed a very good prediction of DO through ECOlab.

The locations of velocity and DO concentration measurements were recorded with a nominal horizontal position accuracy of 0.005 m using a Magellan ProMark3 Thales GPS although boat drift along the mooring line during data collection increased positioning uncertainty. Also, vegetation at the bottom of RSPII made data collection challenging, especially for velocity data collection using a bottom-mounted ADCP. As such, it should be acknowledged that uncertainties were involved in the observed data. For the water quality model, even though some of the constants input for environmental processes were calibrated using the experimental data and literature values,

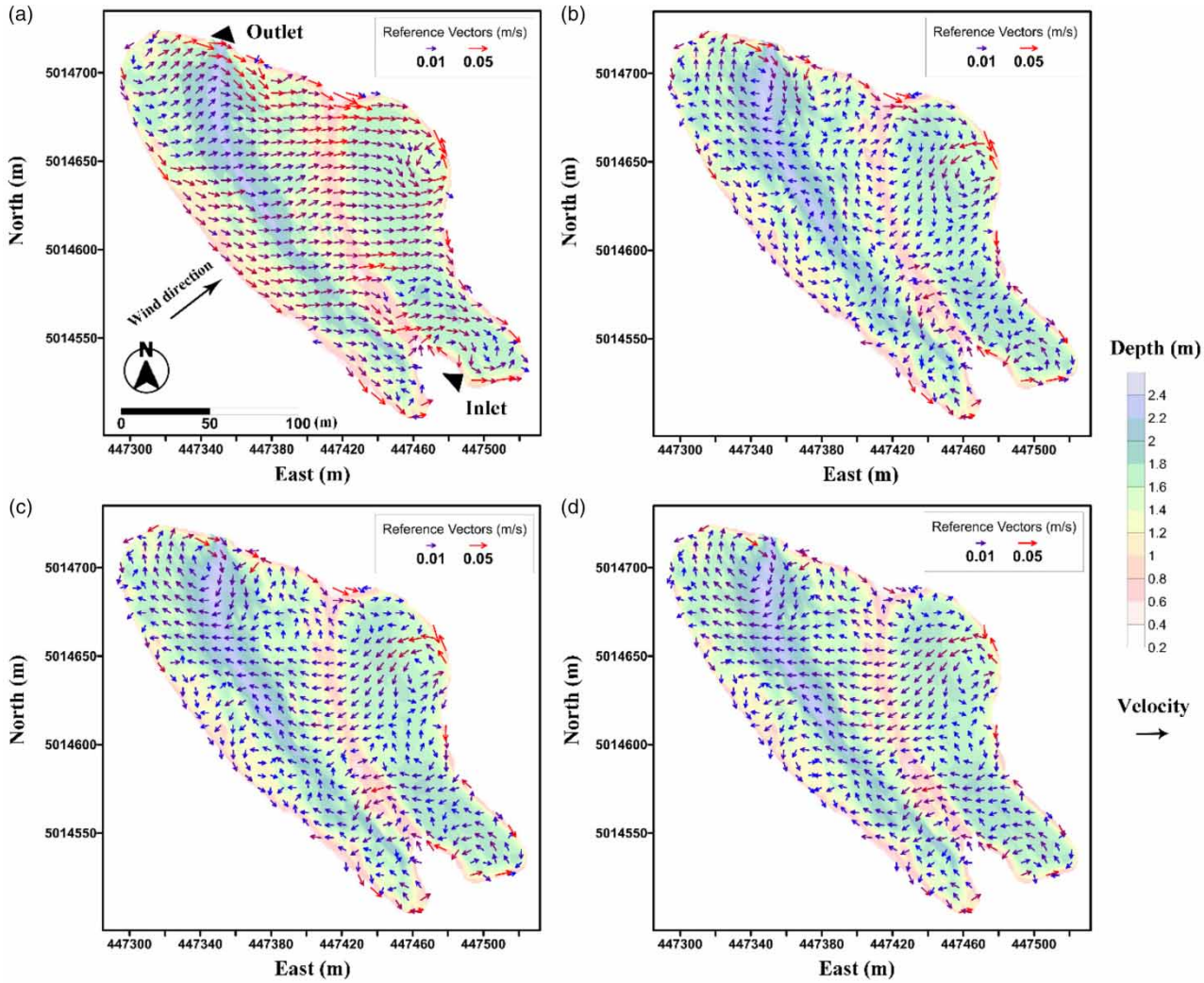

Figure 7 | Simulated velocity results at RSPII on 25 August 2015, using MIKE 3 at layers of (a) 10 (surface), (b) 7, (c) 4 and (d) 1 (bottom).

uncertainties still existed due to the unique environment of RSPII. Regardless, overall the model validation was satisfactory, suggesting that the model can be applied to evaluate mixing under various wind conditions.

Numerical flow and DO simulation as a function of wind

Figure 7 illustrates simulated velocity magnitudes and directions at four specific layers at RSPII. In the σ-coordinate system, MIKE 3 generates layers evenly in the vertical at each mesh cell depending on the total depth of each mesh cell. Consequently, layer thickness is smaller at mesh cells with less total water depth. Although the same layer does not represent the exact same depth in the figure, larger layer numbers indicate layers closer to the water surface. For example, layer 10 is the layer that was closest to the surface and, to the contrary, layer 1 represents the one that was in proximity to the bottom. At the surface layer, flow directions correlated with downwind directions, and it was observed that the larger simulated velocity magnitudes were caused by wind friction. Wind had a stronger impact on shallower bathymetry (Coman & Wells 2012), and higher velocity magnitudes were observed at the surface at locations with the smaller total water depth. Conversely, countercurrent flow in proximity to the bottom of the pond (layer 1) was oriented in the opposite direction to surface velocities due to energy maintenance and mass conservation (Wu & Tsanis 1995). The MIKE 3 simulation

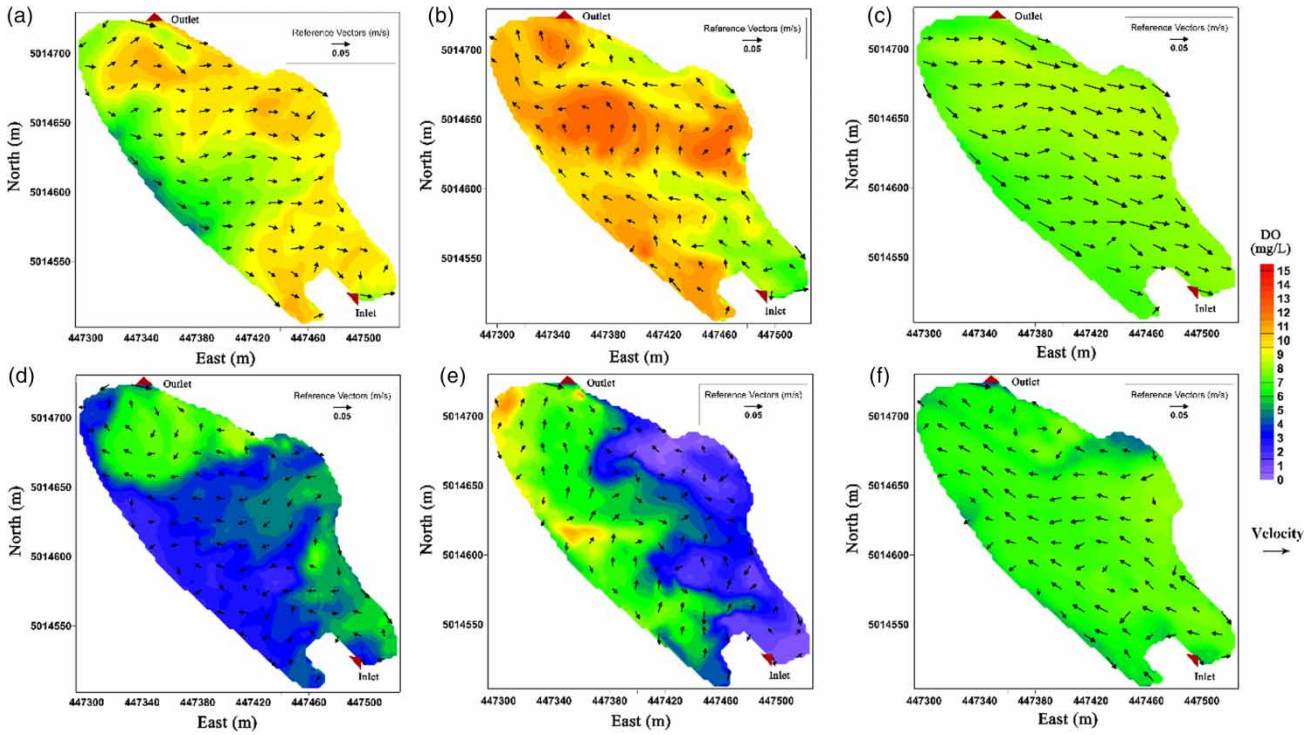

Figure 8 | Simulated velocity and DO results on 25 August 2015 (a) and (d), one low-wind day (b) and (e) and one high-wind day (c) and (f) at the surface layer 10 (a)–(c) and bottom layer 1 (d)–(f).

of opposite directions of surface and bottom flow is similar to the ADCP-acquired observations. This further suggests that wind-driven flow is the main current in RSPII in summer months because of the minimal inflow. Complex circulation cells were generated, especially below the surface layer (Figure 7(b)–7(d)), under certain wind conditions due to wind momentum, fluid viscosity, wave–current interaction and irregular bathymetry (Signell *et al.* 1990; Kachhwal *et al.* 2012). With the upwelling current created by the countercurrent flow at depth at the southeastern border, a pond-scale upwelling circulation was produced by the wind-driven flow, which indicates that hydrodynamic mixing was achieved by wind-driven circulation.

Figure 8(a) and 8(d) show that DO spatial distribution at both surface and bottom layers changed with wind-produced current at RSPII. A segment of higher DO concentrations (approximately 9.00 mg/L) was predicted from the south inlet to north forebay, along with the southeast portion of the pond, due to better replenishing generated by spanwise flows close to the surface. Lower DO between 0.0 and 4.0 mg/L was simulated at depth in the main body of RSPII with exception of the area south of the outlet where near-bed circulation formed a circle of higher DO concentrations of 7.0 mg/L. Due to the downward current generated at the east border of the forebay, DO from the surface supplied the forebay bottom. To the contrary, low DO near the bed at the southwest was raised to the surface through the upward momentum created by pond-scale circulation.

Under the same chemical and hydraulic set-up, a low-wind day and a high-wind day were also simulated. These wind conditions were defined as such in comparison to the moderate wind condition of 25 August 2015, based on the wind data collected from Ottawa International Airport. The flow field under light wind conditions with the average wind speed of 1.15 m/s is shown in Figure 8(b) and 8(e). Decreased wind speed had a greater impact on current directions than velocity magnitudes, which is supported by the findings of Andradóttir & Mortamet (2016). Due to the decrease of wind speed, the overturning circulation weakened, which allowed the development of a stronger vertical stratification (Dumas *et al.* 2012) and caused

hypoxic conditions, defined as DO concentration less than 2.00 mg/L, to be simulated at the bottom of the forebay. Low DO in natural lakes or ponds is likely due to decomposition of dead algae and aerobic microbial activities (Torno *et al.* 2013). With the lack of circulation, anaerobic conditions can be formed, resulting in odour issues and reduced water quality. Under more intense wind conditions of 4.38 m/s average wind speed (Figure 8(c) and 8(f)), higher flow speed was generated at both depths, and a stronger pond-scale circulation was generated with downwind current at surface and countercurrent flow at depth. As such, DO stratification was prevented by stronger circulation, which was created by upwelling windward lower DO at depth and downwelling leeward higher concentrations of

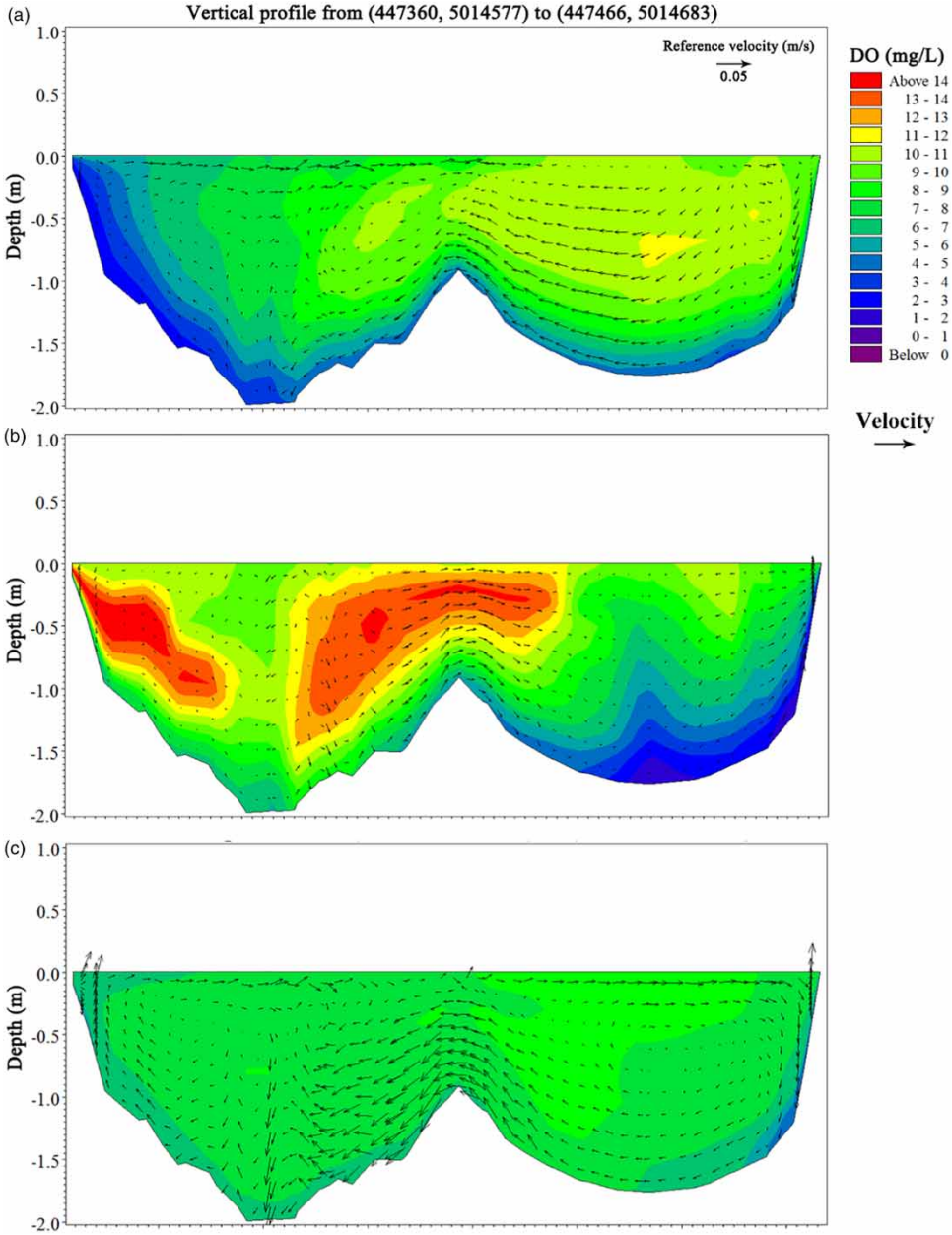

Figure 9 | Vertical profiles of DO concentrations with simulated cross-section velocities on (a) 25 August 2015, (b) one low-wind day and (c) one high-wind day.

surface DO (Dumas *et al.* 2012). Although Andradóttir & Mortamet (2016) reported wind-produced vertical mixing, short-circuiting and basin scale mixing decreased mean residence time, which may have led to reduced water quality. The present model demonstrates that typical high-wind conditions lead to full mixing, sufficient to eliminate hypoxic zones in proximity to the bed.

Figure 9 provides cross-sectional views of DO stratification along the crosswind direction under three wind conditions. With the wind conditions present on 25 August 2015 (Figure 9(a)), stronger countercurrent flow generated from downwelling current at the east border led to higher DO concentrations within the upper water column in the forebay. Comparing with the vertical profile under low-wind conditions (Figure 9(b)), lower DO concentrations were pushed towards the west bank through the countercurrent flow at depth (Figure 9(a)). Microalgae at 0.50 m depth have higher productivity with respect to photosynthesis (Sutherland *et al.* 2014). As such, higher DO was observed at depths ranging from 0.50 to 1.00 m in low-wind conditions, where less mixing and stronger stratification occurred. Figure 9(c) demonstrates a fully mixed cross-section in high-wind conditions. Neither hypoxic conditions nor dead zones were observed even at depth. Stronger downwind current was produced at the forebay surface comparing with smaller wind speed conditions (Figure 9(a)), resulting in both larger downwelling flow in the forebay and stronger upwelling current at the west border in the main pond. The average DO concentrations in this fully mixed condition were around 7.00 mg/L at all depths. Hence, complete mixing is achievable by wind. Overall, with the significant contribution of wind-induced current, hypoxic zones at depth can be prevented by upwelling circulation.

CONCLUSIONS

A three-dimensional MIKE 3 model was carried out to investigate the characteristics of wind-induced hydraulics and its impact on DO concentrations in a shallow SWP (maximum depth <2.5 m). Uniquely, the MIKE 3 ECOlab biogeochemical water quality module was parameterized in part using rate constants determined in the laboratory from samples collected in the SWP. Validation of the hydrodynamic model was challenging due to the constraint of very small velocity magnitudes within the domain. Despite minimal currents, bottom-mounted ADCP measurements provided current speed and directions within the water column, which allowed for convincing validation of the MIKE 3 wind-driven flow predictions. Spatially distributed SOD and Secchi disk depth are sensitive parameters for DO modelling in small and complex regions according to the current study. The hydrodynamic model suggested that a wind-dominated circulation was generated even with moderate wind speed, and it also conclusively simulated near-bed countercurrents, which were in the opposite direction of the surface wind-generated flow. The DO model results demonstrated that complete mixing can be produced by higher wind speed, due to the fact that hypoxic water at depth was carried to the surface and possibly re-oxygenated by upwelling circulation and mixing at the surface. Stronger DO stratification was generated with lower wind speed and hypoxic conditions accumulated at depth in the forebay where most of the sedimentation (higher SOD) occurred. The study demonstrated that pond-scale mixing was first initiated in the downwind water column and that lower DO concentrations could be transported following countercurrent flow at depth. As such, an SWP forebay should be preferentially placed in the downwind direction to benefit from the wind-induced flow and avoid the potential accumulation of hypoxia within the water column. These results highlight that wind-driven currents could be important to pond hydraulics within a small shallow water system. Wind-generated circulation was able to cause full mixing with a slightly higher wind speed.

REFERENCES

Andradóttir, H. Ó. & Mortamet, M.-L. 2016 Impact of wind on storm-water pond hydraulics. *Journal of Hydraulic Engineering* **142** (10), 04016034.

APHA-AWWA-WEF 2012 *Standard Methods for the Examination of Water and Wastewater* (L. Clesceri, A. Greenberg & A. Eaton, eds). APHA, AWWA, WEF, Washington, DC.

Behera, P. K. & Teegavarapu, R. S. V. 2014 Optimization of a stormwater quality management pond system. *Water Resources Management* **29** (4), 1083–1095.

Bentzen, T. R., Larsen, T. & Rasmussen, M. R. 2008 Wind effects on retention time in highway ponds. *Water Science and Technology* **57** (11), 1713–1720.

Butts, T. A. & Evans, R. L. 1979 *Sediment Oxygen Demand in A Shallow Oxbow Lake*. State Water Survey, Urbana, IL.

Canfield, D. E. & Hodgson, L. M. 1983 Prediction of Secchi disc depths in Florida lakes: impact of algal biomass and organic color. *Hydrobiologia* **99** (1), 51–60.

Chen, L., Delatolla, R., D'Aoust, P. M., Wang, R., Pick, F., Poulain, A. & Rennie, C. 2017 Hypoxic conditions in stormwater retention ponds: potential for hydrogen sulfide emission. *Environmental Technology* **40** (5), 642–653.

Coman, M. A. & Wells, M. G. 2012 Temperature variability in the nearshore benthic boundary layer of Lake Opeongo is due to wind-driven upwelling events. *Canadian Journal of Fisheries and Aquatic Sciences* **69** (2), 282–296.

D'Aoust, P. M. 2016 *Stormwater Retention Ponds: Hydrogen Sulfide Production, Water Quality and Sulfate-Reducing Bacterial Kinetics*. University of Ottawa, Canada.

D'Aoust, P. M., Delatolla, R., Poulain, A., Guo, G., Wang, R., Rennie, C., Chen, L. & Pick, F. R. 2017 Emerging investigators series: hydrogen sulfide production in municipal stormwater retention ponds under ice covered conditions: a study of water quality and SRB populations. *Environmental Science: Water Research & Technology* **3** (4), 686–698.

D'Aoust, P. M., Pick, F. R., Wang, R., Poulain, A., Rennie, C., Chen, L., Kinsley, C. & Delatolla, R. 2018 Sulfide production kinetics and model of stormwater retention ponds. *Water Science and Technology* **77** (10), 2377–2387.

Delatolla, R. & Babarutsi, S. 2005 Parameters affecting hydraulic behavior of aerated lagoons. *Journal of Environmental Engineering* **131** (10), 1404–1413.

DHI 2012 MIKE 21 & MIKE 3 FLOW MODEL FM, Hydrodynamic and Transport Module Scientific Documentation.

DHI 2017 MIKE ECO Lab.

Dufresne, C., Duffa, C. & Rey, V. 2014 Wind-forced circulation model and water exchanges through the channel in the Bay of Toulon. *Ocean Dynamics* **64** (2), 209–224.

Dumas, F., Le Gendre, R., Thomas, Y. & Andréfouët, S. 2012 Tidal flushing and wind driven circulation of Ahe atoll lagoon (Tuamotu Archipelago, French Polynesia) from in situ observations and numerical modelling. *Marine Pollution Bulletin* **65** (10–12), 425–440.

Environment Canada Atmospheric Environment Service 2016 *Canadian Climate Normals*. http://climate.weather.gc.ca/climate_normals/index_e.html.

Fabian, J. & Budinski, L. 2013 Horizontal mixing in the shallow Palic Lake caused by steady and unsteady winds. *Environmental Modeling and Assessment* **18** (4), 427–438.

Fan, C. & Wang, W. S. 2008 Influence of biological oxygen demand degradation patterns on water-quality modeling for rivers running through urban areas. *Annals of the New York Academy of Sciences* **1140**, 78–85.

Ferguson, H. L., O'Neill, A. D. J. & Cork, H. F. 1970 Mean evaporation over Canada. *Water Resources Research* **6** (6), 1618–1633.

Geernaert, G. L. & Plant, W. L. 1990 *Surface Waves and Fluxes. Volume I – Current Theory*. Kluwer Academic, Boston, MA.

German, J., Svensson, G., Gustafsson, L. G. & Vikström, M. 2003 Modelling of temperature effects on removal efficiency and dissolved oxygen concentrations in stormwater ponds. *Water Science and Technology* **48** (9), 145–154.

Ghimire, B. K. 2012 *Investigation of Oxygen Half Saturation Coefficients for Nitrification. ProQuest Dissertations and Theses* (September 2000). http://search.proquest.com.proxy.lib.sfu.ca/docview/918160020?accountid=13800.

Glenn, J. S. & Bartell, E. M. 2010 Evaluating short-circuiting potential of stormwater ponds. In: *World Environmental and Water Resources Congress*. pp. 3942–3951. http://ascelibrary.org/doi/10.1061/41114%28371%29401.

Jamu, D. M., Lu, Z. & Piedrahita, R. H. 1999 Relationship between Secchi disk visibility and chlorophyll a in aquaculture ponds. *Aquaculture* **170** (3–4), 205–214.

Jansons, K. & Law, S. 2007 The hydraulic efficiency of simple stormwater ponds. In: *Rainwater and Urban Design 2007*. p. 452.

Jin, K.-R. & Ji, Z.-G. 2004 Case study: modeling of sediment transport and wind-wave impact in Lake Okeechobee. *Journal of Hydraulic Engineering* **130** (11), 1055–1067.

Józsa, J. 2014 On the internal boundary layer related wind stress curl and its role in generating shallow lake circulations. *Journal of Hydrology and Hydromechanics* **62** (1), 16–23.

Kachhwal, L. K., Yanful, E. K. & Rennie, C. D. 2012 A semi-empirical approach for estimation of bed shear stress in a tailings pond. *Environmental Earth Sciences* **66** (3), 823–834.

Khan, S., Melville, B. W., Shamseldin, A. Y. & Fischer, C. 2013 Investigation of flow patterns in storm water retention ponds using CFD. *Journal of Environmental Engineering* **139** (1), 61–69.

Liang, Q., Borthwick, A. G. L. & Taylor, P. H. 2006 Wind-induced chaotic advection in shallow flow geometries. Part II: non-circular basins wind-induced chaotic advection in shallow flow geometries. Part II: non-circular basins Courants chaotiques induits par le vent en zones peu profondes. Partie II. *Journal of Hydraulic Research* **44** (2), 180–188.

Marsalek, J., Urbonas, B. & Lawrence, I. 2005 Stormwater management ponds. In: *Pond Treatment Technology*. IWA Publishing, London, pp. 433–459.

McEnroe, N. A., Buttle, J. M., Marsalek, J., Pick, F. R., Xenopoulos, M. A. & Frost, P. C. 2012 Thermal and chemical stratification of urban ponds: are they 'completely mixed reactors'? *Urban Ecosystems* **16** (2), 327–339.

Ontario Ministry of the Environment 2003 *Stormwater Management Planning and Design Manual*. Queen's Printer for Ontario, Toronto, ON.

Pang, C. C., Wang, F. F., Wu, S. Q. & Lai, X. J. 2015 Impact of submerged herbaceous vegetation on wind-induced current

in shallow water. *Ecological Engineering* **81**, 387–394. http://dx.doi.org/10.1016/j.ecoleng.2015.04.021.

Pattantyús-Ábrahám, M., Tél, T., Krámer, T. & Józsa, J. 2008 Mixing properties of a shallow basin due to wind-induced chaotic flow. *Advances in Water Resources* **31** (3), 525–534.

Rennie, C. D. & Villard, P. V. 2004 Site specificity of bed load measurement using an acoustic Doppler current profiler. *Journal of Geophysical Research: Earth Surface* **109** (F03003), 15.

Rodi, W. 2017 *Turbulence Models and Their Application in Hydraulics*. Routledge, London.

Rolon dos Santos Mérette, M. 2012 *Primary Production and Nutrient Dynamics of Urban Ponds*. Université d'Ottawa/University of Ottawa.

Rong, N. & Shan, B. 2016 Total, chemical, and biological oxygen consumption of the sediments in the Ziya River watershed, China. *Environmental Science and Pollution Research* **23** (13), 13438–13447.

Signell, R. P., Beardsley, R. C., Graber, H. C. & Capotondi, A. 1990 Effect of wave-current interaction on wind-driven circulation in narrow, shallow embayments. *Journal of Geophysical Research: Oceans* **95** (C6), 9671–9678.

Simpson, M. R. 2001 *Discharge Measurements Using A Broad-Band Acoustic Doppler Current Profiler*. U.S. Department of the Interior, U.S. Geological Survey, Reston.

Sutherland, D. L., Turnbull, M. H. & Craggs, R. J. 2014 Increased pond depth improves algal productivity and nutrient removal in wastewater treatment high rate algal ponds. *Water Research* **53**, 271–281.

Tilzer, M. M. 1988 Secchi disk – chlorophyll relationships in a lake with highly variable phytoplankton biomass. *Hydrobiologia* **162** (2), 163–171.

Torno, H. C., Marsalek, J. & Desbordes, M. 2013 *Urban Runoff Pollution*. Springer Science & Business Media, New York.

Tu, Y. T., Chiang, P. C., Yang, J., Chen, S. H. & Kao, C. M. 2014 Application of a constructed wetland system for polluted stream remediation. *Journal of Hydrology* **510**, 70–78.

USEPA 2004 *Stormwater Best Management Practice Design Guide Volume 3: Basin Best Management Practices*, Edison, NJ.

USEPA 2009 *Stormwater Wet Pond and Wetland Management Guidebook*. United States Environmental Protection Agency, Washington, DC.

Wang, W. 1980 Fractionation of sediment oxygen demand. *Water Research* **14** (6), 603–612.

Wium-Andersen, T., Nielsen, A. H., Hvitved-Jacobsen, T. & Vollertsen, J. 2012 Modeling nutrient and pollutant removal in three wet detention ponds. In: *Urban Environment*. Springer, Dordrecht, pp. 237–248.

Wium-Andersen, T., Nielsen, A. H., Hvitved-Jacobsen, T., Brix, H., Arias, C. A. & Vollertsen, J. 2013 Modeling the eutrophication of two mature planted stormwater ponds for runoff control. *Ecological Engineering* **61**, 601–613.

Wu, J. 1980 Wind-stress coefficients over sea surface near neutral conditions – a revisit. *Journal of Physical Oceanography* **10** (5), 727–740.

Wu, J. & Tsanis, I. K. 1995 Numerical study of wind-induced water currents. *Journal of Hydraulic Engineering* **121** (5), 388–395.

Zounemat-Kermani, M., Scholz, M. & Tondar, M. M. 2015 Hydrodynamic modelling of free water-surface constructed storm water wetlands using a finite volume technique. *Environmental Technology* **36** (20), 2532–2547.

First received 22 January 2019; accepted in revised form 27 May 2019. Available online 17 June 2019